The stereodynamic properties of the F + HO (v, j) → HF + O reaction on ^{1}A′ and ^{3}A′ potential energy surfaces by quasi-classical trajectory calculations: Initial excitation effect (v =1–3, j = 0 and v = 0, j =1–3)*

Zhao Dan(赵 丹)[a)b)], Chu Tian-Shu(楚天舒)[b)c)†], and Hao Ce(郝 策)[a)]

[a)] School of Chemical Engineering, Dalian University of Technology, Dalian 116023, China

[b)] State Key Laboratory of Molecular Reaction Dynamics, Dalian Institute of Chemical Physics, Chinese Academy of Sciences, Dalian 116023, China

[c)] Institute for Computational Sciences and Engineering, Laboratory of New Fiber Materials and Modern Textile, the Growing Base for State Key Laboratory, Qingdao University, Qingdao 266071, China

(Received 5 September 2012; revised manuscript received 7 November 2012)

The stereodynamic properties of the F + HO (v, j) reaction are explored by quasi-classical trajectory (QCT) calculations performed on the ^{1}A′ and ^{3}A′ potential energy surfaces (PESs). Based on the polarization-dependent differential cross sections (PDDCSs) and the angular distributions of the product angular momentum with the reactant at different values of initial v or j, the results show that the product scattering and product polarization have strong links with initial vibrational–rotational numbers of v and j. The significant manifestation of the normal DCSs is that the forward scattering gradually becomes predominant with the initial vibrational excitation increasing, and the scattering angle of the HF product taking place on the ^{3}A′ potential energy surface is found to be more sensitive to the initial value of v. The product orientation and alignment are strongly dependent on the initial rovibrational excitation effect. With enhancement in the initial rovibrational excitation effect, there is an overall decrease in the product orientation as well as in the product alignment either perpendicular to the reagent relative velocity vector $\boldsymbol{k}$ or along the direction of the y axis, for which the initial rotational excitation effect is much more noticeable than the vibrational excitation effect. Moreover, the initial rovibrational excitation effect on the product polarization is more pronounced for the ^{3}A′ potential energy surface than for the ^{1}A′ potential energy surface.

Keywords: stereodynamics, quasi-classical trajectory, rotational excitation, vibrational excitation

PACS: 34.10.+x, 34.50.Lf, 31.15.xv **DOI:** 10.1088/1674-1056/22/6/063401

1. Introduction

The HOF system has relatively simple electronic structure in the HOX (X = halogen) family. As one of the model systems of open shell reactions, the HOF system has received more and more attention in recent decades.[1–9] In 2000, Kornweitz and Persky[4] constructed three-center semi-empirical potential energy surfaces for both the F + H_2O and the F + OH reactions. Since 2004, Gomez–Carrasco *et al.*[10–13] have successively gained a series of accurate potential energy surfaces of the HOF system, including the ground singlet 1^1A′, the triplet 1^3A″ and the two excited triplets of 2^3A″ and 1^3A′. All triplet potential energy surfaces have been asymptotically correlated with the F(^{2}P) + HO($^2\Pi$) reactant arrangement,[10–12] while the singlet one is correlated with the O(^{1}D) + HF($^1\Sigma^+$) reactant channel.[13] Then, based on those potential energy surfaces (PESs), insight into the dynamics and kinetics of the HOF reactive system has been provided with a series of theoretical studies.[14–22]

Quantum and quasi-classical methods are popular ones in dynamical studies of chemical reactions. One of the most successful quasi-classical trajectory (QCT) computational codes has been developed by Han's group,[23–27] which is motivated by the intention to interpret their experimental observations including product alignment of chemical reactions. The reliability of this QCT code has been tested and confirmed in its extensive applications in triatomic systems.[28–38]

For the HFO system, there are fewer theoretical studies about the H + FO reaction. The reaction probabilities, integral cross-section and rate constant of this reaction have been investigated on both the 1^3A′ and the 1^3A″ potential energy surfaces (PESs) by Gogtas *et al.*[8,21,22] The stereodynamics of the H + FO reaction have been studied[39–44] but none of these studies dealt with the initial ro-vibrational excitation effect on its stereodynamics, except for a previous work by Meng *et al.*[45] on the ^{3}A′ electronic state. Here, we report on our QCT investigation on the initial ro-vibrational excitation effect for the title reaction on the other two separate electronic states of ^{1}A′ and ^{3}A′.

The polarization-dependent differential cross sections (PDDCSs) and the angular distributions of the product rotational angular momentum for the F + HO (v, j) reaction are shown and discussed in the following section. The collision

*Project supported by the National Natural Science Foundation of China (Grant Nos. 10874096 and 20633070) and the Natural Science Foundation of Qingdao University, China (Grant No. 063-06300510).

†Corresponding author. E-mail: tschu@dicp.ac.cn; tschu008@163.com

© 2013 Chinese Physical Society and IOP Publishing Ltd

energy is chosen to be 0.6 eV and these results are obtained by running batches of 10^5 trajectories in integration steps of 0.1 fs.[46] The trajectories are started at a distance of 20 Å (1 Å = 0.1 nm) between the hydrogen atom and the center-of-mass of HO. To reveal the initial excitation effect, the calculations have been performed for the initial ro-vibrational quantum numbers of $v = 1, 2, 3$, $j = 0$, and $v = 0$, $j = 1, 2, 3$. The details of the computational method and code have been described previously.[23–25,47] And a figure showing the relations among reagent relative velocity $\boldsymbol{k}$, product relative velocity $\boldsymbol{k}'$, and product rotational angular momentum $\boldsymbol{j}'$ can be found in Ref. [46]. As usual, we use θ_t to denote the scattering angle between $\boldsymbol{k}$ and $\boldsymbol{k}'$, θ_r (i.e., the angle between $\boldsymbol{k}$ and $\boldsymbol{j}'$) and φ_r (i.e., the dihedral angle between the $\boldsymbol{k}'$–$\boldsymbol{k}$ plane and the $\boldsymbol{k}$–$\boldsymbol{j}'$ plane) to denote the azimuthal angles that determine the spatial direction of $\boldsymbol{j}'$ within a center-of-mass frame.

2. Results and discussion

To gain a mechanistic insight into the F + HO $(v, j) \rightarrow$ HF + O reaction, the values of $PDDCS_{00}$ of the product HF with different reagent initial ro-vibrational excitations, for the $^1A'$ and $^3A'$ electronic states, are first shown in Fig. 1. At $v = 0$ and $j = 0$, the forward scattering is preponderant in characteristic on the $^1A'$ PES, while in the triplet state the sideway scattering and the back-scattering are visible. As seen in the left top panel of Fig. 1, products retain forward scattering with reagents' vibrational excitation on the $^1A'$ PES, and with the increase in the initial vibrational quantum number v, the degree of forward scattering is overall rapidly enhanced. While in the $^3A'$ state, as depicted in the left bottom plot of Fig. 1, the product tends to become forward scattered at a high vibrational level and the increase in forward scattering is clearly intense with v increasing. The right two panels in Fig. 1 describe the scattering directions of the product on the two PESs for different rotational excitation states. In this case, the initial rotational quantum number j influences the product scattering only a little compared with the former one, suggesting that the scattering distribution is less sensitive to the initial rotational number on these two PESs. It is further found that the product scattering taking place on the $^3A'$ PES changes more noticeably than on the A' PES with the initial vibrational excitation effect. This can be attributed to the difference in PES characteristic between the two electronic states: the most noteworthy characteristic of the $^1A'$ PES is the deep well which is located in the F + HO channel and corresponds to a bent equilibrium geometry with a fitted OHF angle of 50.5°; its minimum energy is about 2.1 eV below the F + HO asymptote. This PES feature indicates an insertion reaction mechanism where the O atom is inserted into the HF bond. The $^1A'$ PES also has a shallow van der Waals well of 0.3 eV located in the HF + O channel and a transition state with an energy of 0.375 eV in the F + HO channel.[13] On the other hand, the $^3A'$ PES has a collinear transition state with an energy barrier of 0.276 eV, and a shallow well of 0.04 eV located in the F + HO channel. In addition, this triplet PES does not have a van der Waals well in the F + HO channel.[12] As such, the increase of vibrational quantum number is helpful for the products of a triplet state to leap over the barrier and to illustrate stronger forward scattering.

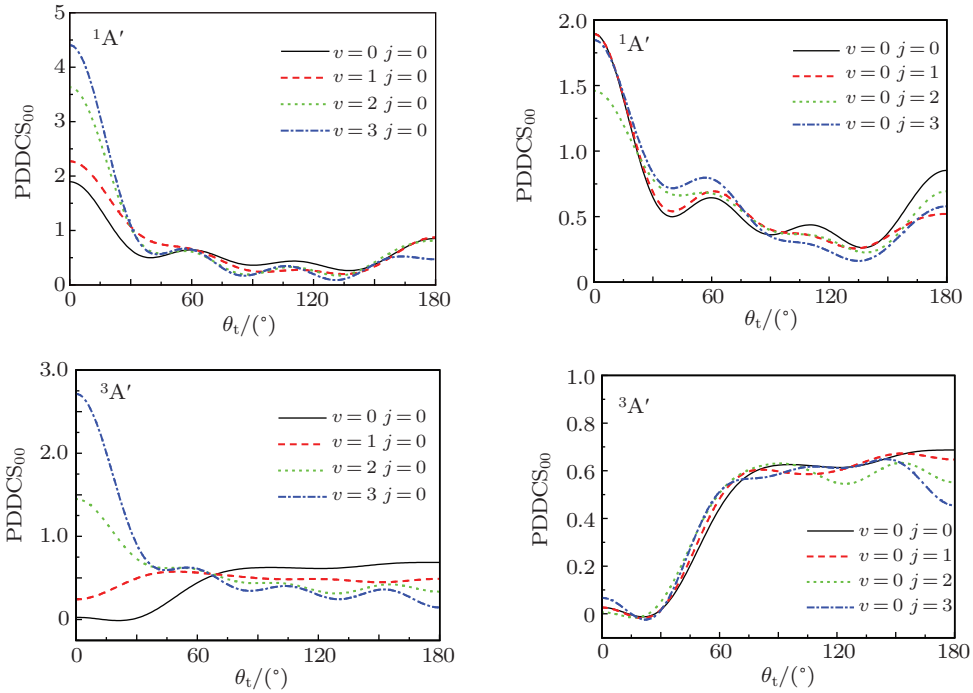


Fig. 1. (color online) The values of $PDDCS_{00}$s of F + HO ($v = 1, 2, 3$, $j = 0$ and $v = 0$, $j = 1, 2, 3$) → HF + O on the $^1A'$ and $^3A'$ PESs versus θ_t. Solid line, dashed line, dotted line, and, dash–dot line correspond to v or $j = 0, 1, 2, 3$, respectively. The top panels are on the $^1A'$ PES, and the bottom panels are on the $^3A'$ PES.

The other PDDCSs can reflect the alignment of the product rotational angular momentum. In Fig. 2, we present our calculated values of $PDDCS_{20}$ for F + HO ($v = 1, 2, 3$, $j = 0$ and $v = 0$, $j = 1, 2, 3$) $\rightarrow$ HF + O on the $^1A'$ and $^3A'$ PESs versus θ_t. Solid line, dashed line, dotted line, and dash–dot line correspond to v or $j = 0, 1, 2, 3$, respectively. As can be seen from the top two panels of Fig. 2, the product rotational angular momentum is more anisotropic with the increase of reagent initial vibrational/rotational number on the $^1A'$ PES. Moreover, the behavior of $PDDCS_{20}$ is of mirror symmetry with respect to that of $PDDCS_{00}$ generated on the $^1A'$ PES, which shows that the alignment of product rotational angular momentum is perpendicular to the reagent relative velocity $\boldsymbol{k}$. Comparing the two initial excitations, the initial rotational excitation has a little influence on the polarization of the product in the whole range of scattering angle θ_t. On the $^3A'$ PES, the product rotational angular momentum also shows more anisotropic when the initial vibrational excitation is high, and the tendency of $PDDCS_{20}$ is similar to that of $^1A'$ PES with the increase of v where the degree of anisotropy is stronger. Under the initial rotational excitation the polarization of the product is strongest when the scattering angle is about 150° on the $^3A'$ PES. Thus, the more pronounced initial vibrational effect is found in the enhancing of the polarizations of products on the two PESs. For the initial rotational excitation effect, it plays a less influential role in affecting the distribution of $PDDCS_{20}$.

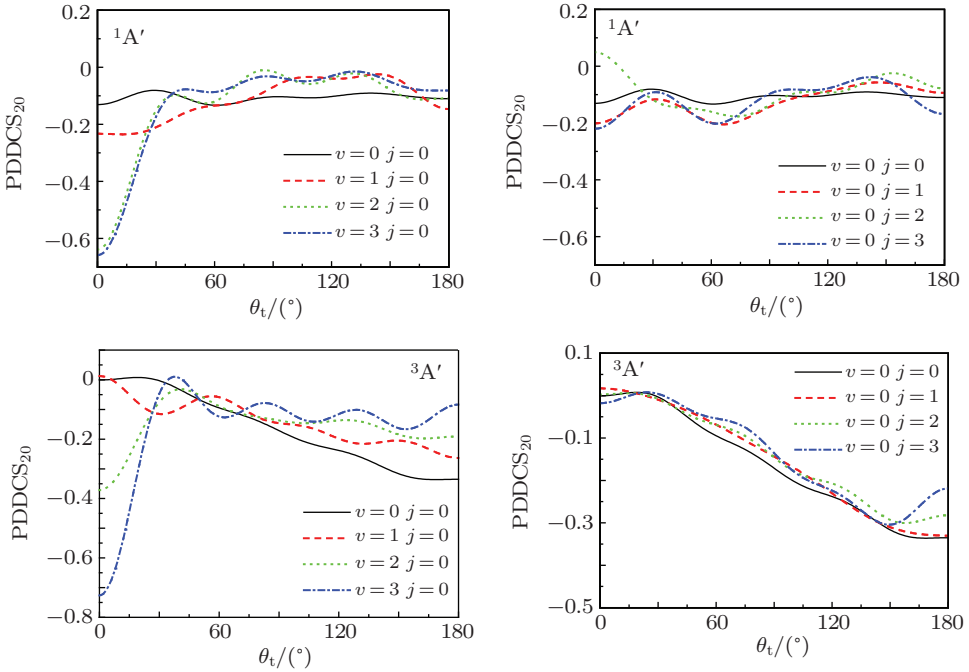


Fig. 2. (color online) The values of $PDDCS_{20}$s of F + HO ($v = 1, 2, 3$, $j = 0$ and $v = 0$, $j = 1, 2, 3$) $\rightarrow$ HF + O on the $^1A'$ and $^3A'$ PESs versus θ_t. Solid line, dashed line, dotted line, and dash–dot line correspond to v or $j = 0, 1, 2, 3$, respectively. The top panels are on the $^1A'$ PES, and the bottom panels are on the $^3A'$ PES.

Figure 3 shows the values of $PDDCS_{22+}$ of F + HO (v, j) $\rightarrow$ HF + O on the $^1A'$ and $^3A'$ PESs versus θ_t for the cases of $v = 1, 2, 3$, $j = 0$ and $v = 0$, $j = 1, 2, 3$. The distribution becomes more anisotropic in the whole range of the scattering angle with the reagent in $v \neq 0$. On the $^1A'$ potential energy surface, around the scattering angle of 30°, the value of $PDDCS_{22+}$ is approximately -0.6124 in $v = 1$ excitation state. Based on the limiting values of the alignment parameters, the information exposes that the products scattered at this angle tend to align along the direction of the resultant vector of vectors in the y and z directions. The same aligning phenomenon occurs on the $^3A'$ potential energy surface, when the quantum number of vibrational excitation states is 3. These demonstrate that the vibrational excitation effect can influence the azimuthal angle of product rotational angular momentum. Similarly, the initial rotational excitation effect can also influence the distribution of $PDDCS_{22+}$ but to a lesser extent.

In Fig. 4, the curves of $PDDCS_{21-}$ are depicted. From the left top panel of Fig. 4, we can find that most of $PDDCS_{21-}$ is close to zero with the increase of v on the $^1A'$ potential energy surface. This behavior shows that the product is apparently isotropic in the range of scattering angle for the initial vibrational number $v \neq 0$. In the right top panel of Fig. 4, we can find that the distributions vary with rotational number and that there is a minimum peak at the scattering angle about 31° for the highest rotational excitation state on the same poten-

tial energy surface. Thus, on the singlet state as reflected by $PDDCS_{21-}$, the product alignment tends to become isotropic under the initial vibrational excitation, while on the contrary, the initial rotational excitation effect enhances the anisotropic degree of the product rotational angular momentum. For the $^3A'$ potential energy surface, the influence of the initial ro-vibrational quantum number on $PDDCS_{21-}$ can be seen in the bottom of Fig. 4, obviously, the initial vibrational excitation more influences the product alignment depicted by $DDCS_{21-}$ than the initial rotational excitation.

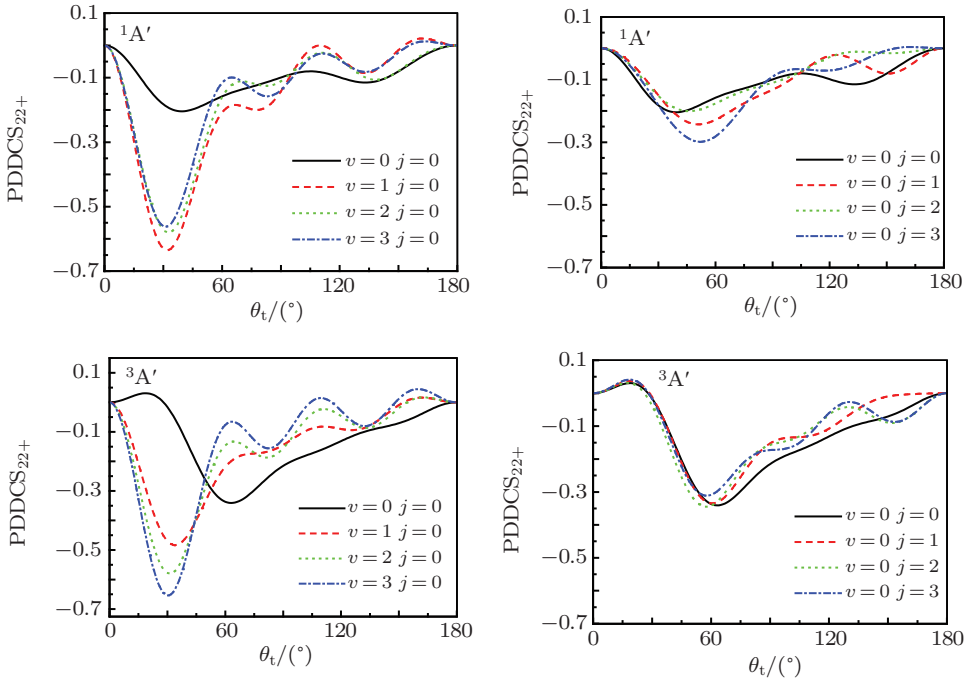


Fig. 3. (color online) Values of $PDDCS_{22+}$s of F + HO ($v = 1, 2, 3$, $j = 0$ and $v = 0$, $j = 1, 2, 3$) → HF + O on the $^1A'$ and $^3A'$ PESs versus θ_t. Solid line, dashed line, dotted line, and dash–dot line correspond to v or $j = 0, 1, 2, 3$, respectively. The top panels are on the $^1A'$ PES, and the bottom panels are on the $^3A'$ PES.

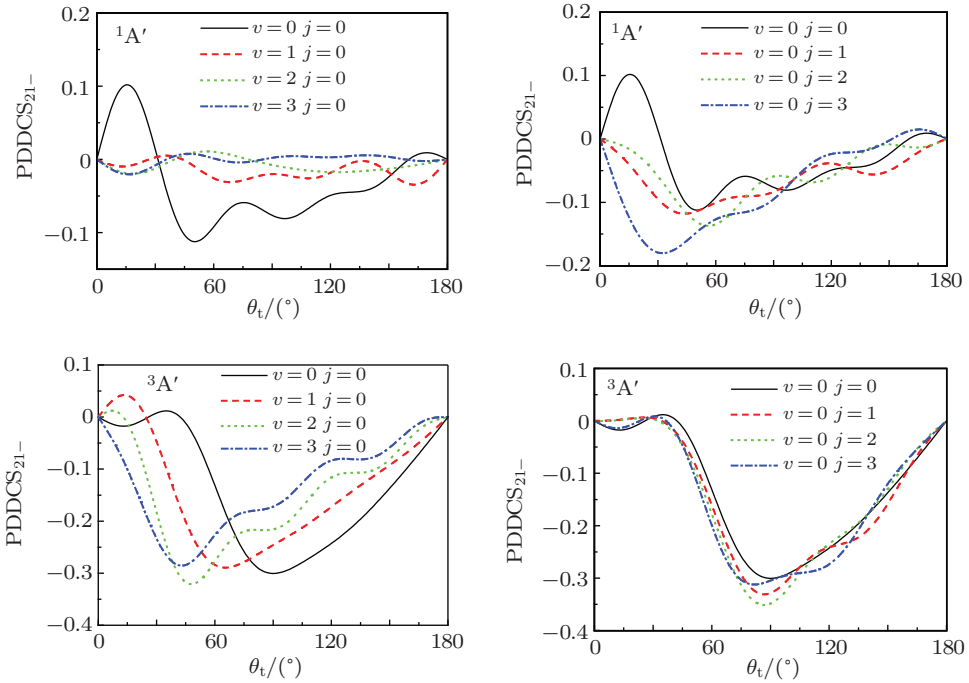


Fig. 4. (color online) Values of $PDDCS_{21-}$s of F + HO ($v = 1, 2, 3$, $j = 0$ and $v = 0$, $j = 1, 2, 3$) → HF + O on the $^1A'$ and $^3A'$ PESs versus θ_t. Solid line, dashed line, dotted line, and dash–dot line correspond to v or j=0, 1, 2, 3, respectively. The top panels are on the $^1A'$ PES, and the bottom panels are on the $^3A'$ PES.

Next, we discuss the $P(\theta_r)$ distribution and $P(\varphi_r)$ distribution. As is well known, the $P(\theta_r)$ distribution and the $P(\varphi_r)$ distribution of the title reaction describe the $\boldsymbol{k}$–$\boldsymbol{j}'$ correlation and the $\boldsymbol{k}$–$\boldsymbol{k}'$–$\boldsymbol{j}'$ correlation, respectively, which also provide an insight into the alignment and orientation of the product. The $P(\theta_r)$ distributions of the F + HO (v, j) reaction on the ^{1}A′ and ^{3}A′ electronic states are shown in Fig. 5 for $v = 0$, $j = 1$, 2, 3, and $j = 0$, $v = 1$, 2, 3. As seen, the maximum values of all the $P(\theta_r)$ distributions are located at $\theta_r = 90°$ and are symmetric with respect to $\theta_r = 90°$. The phenomena illustrate that the product rotational angular momentum vector $\boldsymbol{j}'$ aligns along the direction perpendicular to $\boldsymbol{k}$. Moreover, there is no discrepancy in the trend of the product alignment between the two PESs with the increases of the initial reagent vibrational and rotational quantum numbers. As the reagent initial rotational quantum number increases, the peak of the $P(\theta_r)$ distribution rapidly becomes lower and the distribution becomes broader on both PESs, which demonstrates that the polarization (i.e., alignment perpendicular to $\boldsymbol{k}$) degree of the product HF strongly decreases under the initial rotational excitation effect. In comparison, the $P(\theta_r)$ distributions of the reaction occurring on the two PESs decrease to a much smaller extent with the increase of the initial reagent vibrational quantum number. Thus, the initial rotational excitation effect plays a more important role in weakening the product alignment perpendicular to $\boldsymbol{k}$. To quantify the above conclusion, we further compute the expectation value of $\langle P_2(\cos\theta_r)\rangle$ on the ^{1}A′ PES as an example. The expectation value of $\langle P_2(\cos\theta_r)\rangle$ of the F + HO ($v = 0$, $j = 0$) → HF + O reaction is −0.4451, while those of $\langle P_2(\cos\theta_r)\rangle$ are −0.4351, −0.4231, and −0.4177 for the initial reagent vibrational quantum numbers of 1, 2, and 3, respectively. This further evidences that the product alignment is weaker for the higher vibrational excitation state, and this is also consistent with the above result of PDDCS$_{22+}$ distribution on the ^{1}A′ state. In addition, as clearly seen from Fig. 5, initial reagent rotational quantum number in fact has much larger influence on the product rotational alignment. Especially on the ^{3}A′ PES, as j increases, the peak rapidly shifts toward a lower value. Those details show that the initial high j value could more intensively weaken the product rotational alignment on the ^{3}A′ PES. Here, our results confirm this by showing that the $P(\theta_r)$ distribution is dependent on not only the PES but also the reagent initial ro-vibrational quantum number.

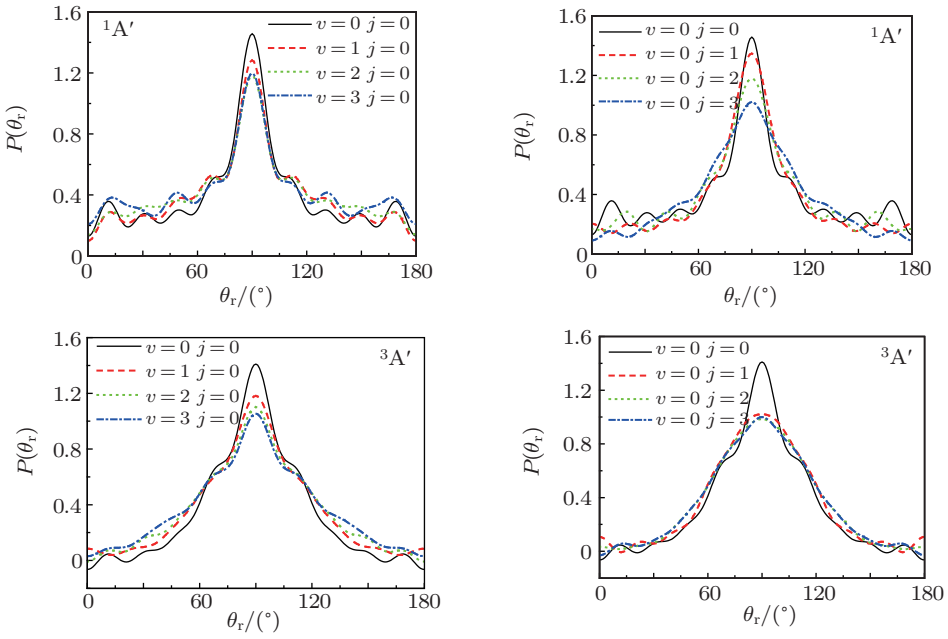


Fig. 5. (color online) Distributions of $P(\theta_r)$ for the HF products from the F + HO ($v = 1$, 2, 3, $j = 0$ and $v = 0$, $j = 1$, 2, 3) → HF + O reactions on the ^{1}A′ and ^{3}A′ PESs.

We also calculate the $P(\theta_r)$ distributions for the isotopic reactions of F + DO ($v = 1$, 2, 3, $j = 0$ and $v = 0$, $j = 1$, 2, 3) → DF + O in order to provide some information about isotope effect. The calculation results are presented in Fig. 6. Comparing Fig. 6 with Fig. 5, prominent differences are found for the product polarization on the ^{1}A′ electronic state. First, the product polarization behavior on this electronic state, namely, the product alignment perpendicular to $\boldsymbol{k}$, almost disappears in the DF products out of the isotopic reaction with initial ro-vibrational states of $v = 0$ and $j = 0$, 1, 2, 3, but excitation of the reagent molecules to higher vibrational levels induces the DF products gradually, showing the aligned tendency perpendicular to $\boldsymbol{k}$. Second, the polarization tendency with the quantum numbers of v, j is also quite different for the two reactions of F + HO and F + DO on the ^{1}A′ state. In the isotopic reaction, the degree of the product alignment, though relatively weak, increases as v increases while it is rather insensitive to the quantum number j. In contrast, the product alignment in

the F + HO reaction is weakened as v and j increase. While for the product alignment on the triplet state, the differences are not very remarkable between F + HO and F + DO, because isotope substitution only leads to a slight decrease in product alignment while the trend of product alignment with v, j remains the same as that of F + HO. Hence, the results we discussed here demonstrate that for the $P(\theta_r)$ distribution and the product alignment reflected by this distribution, the isotope effect is more pronounced in the singlet electronic state than in the triplet electronic state.

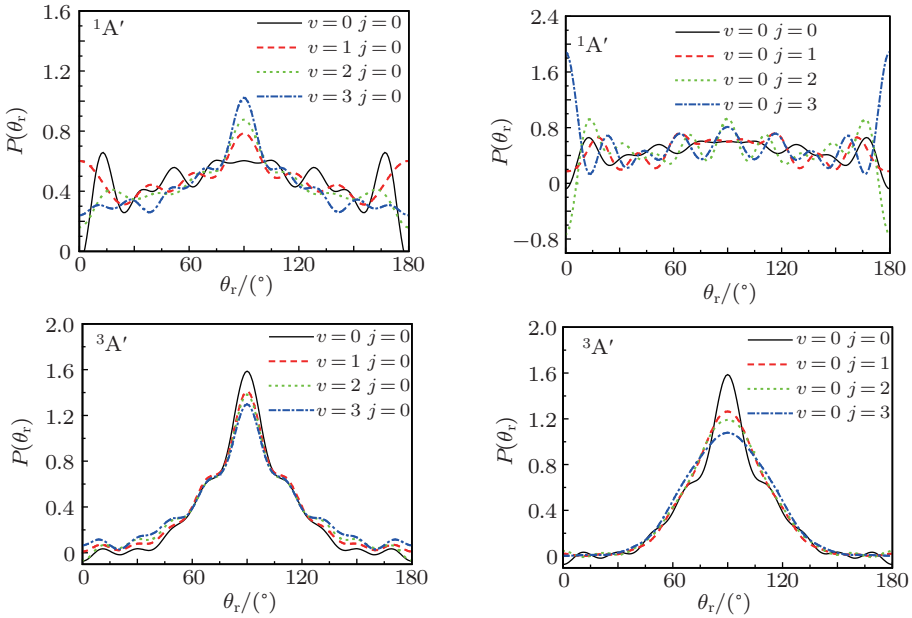


Fig. 6. (color online) Distributions of $P(\theta_r)$ for the DF products from the F + DO ($v = 1, 2, 3$, $j = 0$ and $v = 0$, $j = 1, 2, 3$) → DF + O reactions on the ^{1}A′ and ^{3}A′ PESs.

To further reveal the ro-vibrational excitation effect on the product polarization of F + HO, especially on the product orientation, we calculate the $P(\varphi_r)$ distribution. The results of the $P(\varphi_r)$ distribution are shown in Fig. 7. The discrepancy in product orientation exists clearly between the two PESs: first, at $v = 0$, $j = 0$, the asymmetric feature of the $P(\varphi_r)$ distribution with respect to $\varphi_r = 180^\circ$ indicates that the product on the ^{1}A′ PES is oriented to the positive direction of the y axis while that on the ^{3}A′ PES to the negative direction of the y axis, with stronger product orientation on the triplet PES. In other words, this asymmetric phenomenon reflects a kind of "in-plane" mechanism where the product molecules rotate in a plane parallel to the scattering $\boldsymbol{k}$–$\boldsymbol{k}'$ plane. Second, with the increase of the initial vibrational quantum number v, in the ^{1}A′ state, the peak at 90° shifts down then up while the peak at 270° goes up then down, indicating that excitation of the reagent molecule to the first few vibrational levels may enhance the product orientation but further vibrational excitation will weaken the degree of the product orientation. On the ^{3}A′ PES, though the product remains oriented to the negative direction of the y axis at different vibrational quantum numbers, this behavior, nonetheless, is lessened to some degree due to the initial vibrational excitation. Further, we observe from the right panels in Fig. 7, the influence of j on the product polarization shows a similar pattern for the two PESs where almost all the peaks of the $P(\varphi_r)$ distribution go down with j increasing, indicating the weakening trend in product alignment along the y axis with initial rotational excitation increasing. At $j = 3$, the peak at 270° has nearly half a height as in the case at $j = 0$ on the ^{3}A′ PES, suggesting that the product orientation on this electronic state decreases at a fairly large scale as the reagent reaches a high initial rotational excitation level. According to the commonly used impulse model,[48] which suggests that the impulsive energy of a reactive system is responsible for the asymmetric features of the product rotational angular momentum $\boldsymbol{j}'$, it is very likely that the impulsive energy will drop off with the increase of the initial j value, resulting in the observed weakened product orientation with higher rotational excitation.

Generally, the type of mass combination of a reaction also plays a role in influencing product rotational polarization. In Refs. [23], [26], and [27] the product polarizations on different types of PESs for reactions with different mass combinations were investigated, and the common features of product polarization associated with both mass combination and PES were summarized. For the present heavy–light–heavy (HLH) mass combination, they concluded that a lot of products are scattered at $\varphi_r \leq 180$ on an attractive surface.[26] Our calculation results of $P(\varphi_r)$ on the ^{1}A′ PES also demonstrate this feature, thus the previous finding for HLH mass combination is further supported.

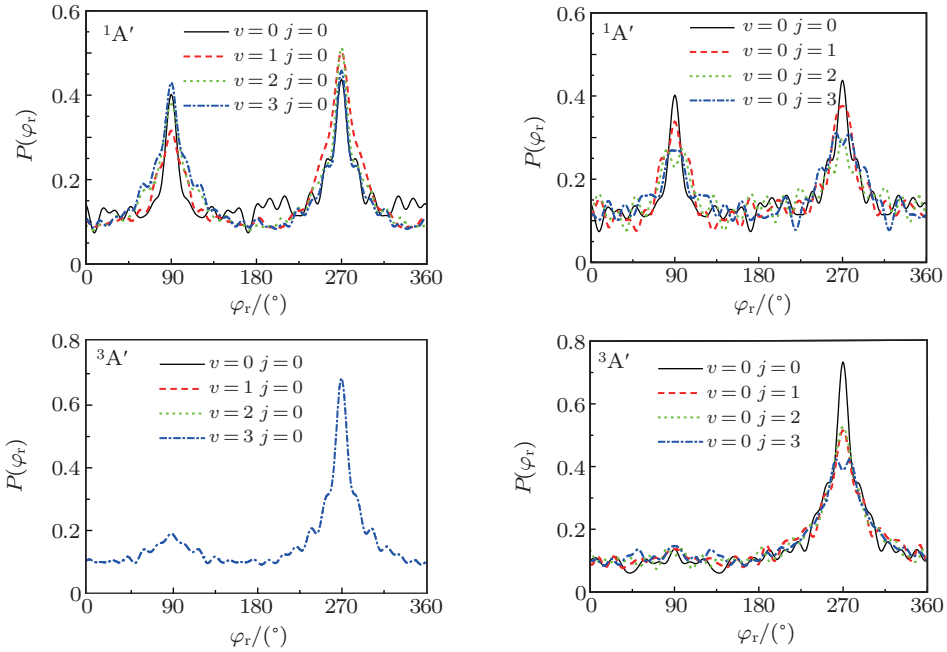


Fig. 7. (color online) Distributions of $P(\varphi_r)$ for HF products from the F + HO ($v = 1, 2, 3$, $j = 0$ and $v = 0$, $j = 1, 2, 3$) → HF + O reactions on the ^{1}A′ and ^{3}A′ PESs.

3. Conclusions

Our investigation focuses on the product scatterings and product rotational polarizations of the title reaction under different initial rotational–vibrational numbers on the ^{1}A′ and ^{3}A′ PESs by QCT calculations. PDDCSs and the distributions of $P(\theta_r)$ and $P(\varphi_r)$ are calculated and discussed. With the increase of the initial v number, the scattering angle of the HF product turns to be smaller and thus the forward scattering is enhanced. This shows that the product scattering is influenced by the initial vibrational excitation effect. The initial rotational excitation shows less effect on the product scattering. Analyses of the other PDDCS distributions demonstrate that the vibrational excitation effect plays a more important role in influencing the polarization-dependent behaviors of the products than the rotational excitation effect. When considering the product polarizations characterized by the distributions of $P(\theta_r)$ and $P(\varphi_r)$, however, the initial rotational excitation has a more pronounced effect than the vibrational effect, especially for the ^{3}A′ PES. And it is found that, overall, these aligned and oriented behaviors decrease as the initial ro-vibrational number increases. This phenomenon indicates that the alignment and orientation of the product is strongly dependent on initial excitation effect. Furthermore, for the two investigated electronic states, the change in the product polarization occurring on the ^{3}A′ PES is more noticeable with the increase of initial v and j values, while the isotope effect is more significant on the ^{1}A′ PES with respect to the $P(\theta_r)$ distribution.

References

[1] Sloan J J, Watson D G, Williamson J M and Wright J S 1981 *J. Chem. Phys.* **75** 1190
[2] Bradforth S E, Arnold D W, Metz R B, Weaver A and Neumark D M 1991 *J. Phys. Chem.* **95** 8066
[3] Dixon R N and Tachikawa H 1999 *Mol. Phys.* **97** 195
[4] Kornweitz H and Persky A 2000 *Chem. Phys. Lett.* **331** 132
[5] Elghobashi N and Gonzalez L 2004 *Phys. Chem. Chem. Phys.* **6** 4071
[6] Neumark D M 2005 *Phys. Chem. Chem. Phys.* **7** 433
[7] Deyerl H J and Continetti R E 2005 *Phys. Chem. Chem. Phys.* **7** 855
[8] Gogtas F 2008 *J. Comput. Chem.* **29** 1889
[9] Zanchet A, Gonzalez-Lezana T, Aguado A, Gomez-Carrasco S and Roncero O 2010 *J. Phys. Chem. A* **114** 9733
[10] Gomez-Carrasco S, Gonzalez-Sanchez L, Aguado A, Paniagua M, Roncero O, Hernandez M L and Alvarino J M 2004 *Chem. Phys. Lett.* **383** 25
[11] Gomez-Carrasco S, Gonzalez-Sanchez L, Aguado A, Roncero O, Alvarino J M, Hernandez M L and Paniagua M 2004 *J. Chem. Phys.* **121** 4605
[12] Gomez-Carrasco S, Roncero O, Gonzalez-Sanchez L, Hernandez M L, Alvarino J M, Paniagua M and Aguado A 2005 *J. Chem. Phys.* **123** 114310
[13] Gomez-Carrasco S, Hernandez M L and Alvarino J M 2007 *Chem. Phys. Lett.* **435** 188
[14] Gonzalez-Sanchez L, Gomez-Carrasco S, Aguado A, Paniagua M, Hernandez M L, Alvarino J M and Roncero O 2004 *J. Chem. Phys.* **121** 309
[15] Gonzalez-Sanchez L, Gomez-Carrasco S, Aguado A, Paniagua M, Hernandez M L, Alvarino J M and Roncero O 2004 *J. Chem. Phys.* **121** 9865
[16] Gonzalez-Sanchez L, Gomez-Carrasco S, Aguado A, Paniagua M, Hernandez M L, Alvarino J M and Roncero O 2004 *Mol. Phys.* **102** 2381
[17] Gomez-Carrasco S and Roncero O 2006 *J. Chem. Phys.* **125** 054102
[18] Chu T S, Zhang H, Yuan S P, Fu A P, Si H Z, Tian F H and Duan Y B 2009 *J. Phys. Chem. A* **113** 3470
[19] Chu T S 2010 *J. Comput. Chem.* **31** 1385
[20] Han B R, Zong F J, Wang C L, Ma W Y and Zhou J H 2010 *Chem. Phys.* **374** 94
[21] Gogtas F, Tutuk R and Kurban M 2010 *J. Comput. Chem.* **31** 2607
[22] Kurban M, Gogtas F, Karabulut E and Tutuk R 2011 *Mol. Phys.* **109** 789
[23] Han K L, He G Z and Lou N Q 1996 *J. Chem. Phys.* **105** 8699

[24] Han K L 1997 *Phys. Rev. A* **56** 4992
[25] Ju L P, Han K L and Zhang J Z 2009 *J. Comput. Chem.* **30** 305
[26] Wang M L, Han K L and He G Z 1998 *J. Chem. Phys.* **109** 5446
[27] Wang M L, Han K L and He G Z 1998 *J. Phys. Chem. A* **102** 10204
[28] Chen M D, Han K L and Lou N Q 2002 *Chem. Phys. Lett.* **357** 483
[29] Chen M D, Han K L and Lou N Q 2003 *J. Chem. Phys.* **118** 4463
[30] Ge M H and Zheng Y J 2011 *Chin. Phys. B* **20** 083401
[31] Chen X Q, Wang M S, Yang C L and Wu J C 2012 *Chin. Phys. B* **21** 023402
[32] Li X H, Wang M S, Pino I, Yang C L and Ma L Z 2009 *Phys. Chem. Chem. Phys.* **11** 10438
[33] Yue X F 2012 *Chin. Phys. B* **21** 073401
[34] Jing X, Yang C L and Wang M S 2012 *Chin. Phys. B* **21** 043101
[35] Hou C Y, Li Y M and Zhao D 2009 *Chem. Phys.* **364** 64
[36] Xu Z H and Zong F J 2011 *Chin. Phys. B* **20** 063104
[37] Han B R, Yang H A, Zheng Y J and Varandas A J C 2010 *Chem. Phys. Lett.* **493** 225
[38] Xu W W and Zhao G J 2012 *Cent. Eur. J. Phys.* **10** 253
[39] Zhao J 2011 *Can. J. Chem.-Rev. Can. Chim.* **89** 650
[40] Zhao J, Xu Y and Meng Q T 2010 *Chin. Phys. B* **19** 063403
[41] Zhao J, Xu Y, Zhao X and Meng Q T 2010 *Sci. China: Chem.* **53** 927
[42] Zhao J, Xu Y, Yue D G and Meng Q T 2009 *Chem. Phys. Lett.* **471** 160
[43] Zhao J, Xu Y and Meng Q T 2009 *J. Phys. B: At. Mol. Opt. Phys.* **42** 165006
[44] Zhao J, Xu Y and Meng Q T 2009 *Can. J. Phys.* **87** 1247
[45] Meng Q T, Zhao J, Xu Y and Yue D G 2009 *Chem. Phys.* **362** 65
[46] Zhao D, Chu T S and Hao C 2012 *J. Mol. Model.* **18** 3283
[47] Zhao D, Zhang T Y and Chu T S 2010 *Can. J. Chem.-Rev. Can. Chim.* **88** 893
[48] Li R J, Han K L, Li F E, Lu R C, He G Z and Lou N Q 1994 *Chem. Phys. Lett.* **220** 281